Field-Angle Dependence Reveals Odd-Parity Superconductivity in CeRh$_2$As$_2$

J. F. Landaeta[1,*] P. Khanenko[1] D. C. Cavanagh[2] C. Geibel[1] S. Khim[1] S. Mishra[3]
I. Sheikin[3] P. M. R. Brydon[4] D. F. Agterberg[5] M. Brando[1] and E. Hassinger[1,6,†]

[1]*Max Planck Institute for Chemical Physics of Solids, 01187 Dresden, Germany*
[2]*Department of Physics, University of Otago, P.O. Box 56, Dunedin 9054, New Zealand*
[3]*Laboratoire National des Champs Magnétiques Intenses (LNCMI-EMFL),
CNRS, UGA, 38042 Grenoble, France*
[4]*Department of Physics and MacDiarmid Institute for Advanced Materials and Nanotechnology,
University of Otago, P.O. Box 56, Dunedin 9054, New Zealand*
[5]*Department of Physics, University of Wisconsin-Milwaukee, Milwaukee, Wisconsin 53201, USA*
[6]*Technical University Munich, Physics Department, 85748 Garching, Germany*

CeRh$_2$As$_2$ is an unconventional superconductor with multiple superconducting phases and $T_c = 0.26$ K. When $H \| c$, it shows a field-induced transition at $\mu_0 H^* = 4$ T from a low-field superconducting state SC1 to a high-field state SC2 with a large critical field of $\mu_0 H_{c2} = 14$ T. In contrast, for $H \perp c$, only the SC1 with $\mu_0 H_{c2} = 2$ T is observed. A simple model based on the crystal symmetry was able to reproduce the phase diagrams and their anisotropy, identifying SC1 and SC2 with even and odd parity superconducting states, respectively. However, additional orders were observed in the normal state which might have an influence on the change of the superconducting state at H^*. Here, we present a comprehensive study of the angle dependence of the upper critical fields using magnetic ac susceptibility, specific heat, and torque on single crystals of CeRh$_2$As$_2$. The experiments show that the state SC2 is strongly suppressed when rotating the magnetic field away from the c axis and it disappears for an angle of 35°. This behavior agrees perfectly with our extended model of a pseudospin triplet state with $\vec{d}$ vector in the plane and hence allows us to conclude that SC2 is indeed the suggested odd-parity state.

I. INTRODUCTION

Odd-parity or (pseudo)spin triplet superconductivity is a rare phenomenon in nature. Only a few materials are promising candidates, including UPt$_3$ [1], the ferromagnetic superconductors UCoGe, URhGe, UGe$_2$ [2], and UTe$_2$ [3]. In these systems, important information on the superconducting (SC) state has come from an investigation of the angle dependence of the critical fields. Theoretically, when spin-orbit coupling is strong, the angle dependence of the Pauli-limiting field H_P offers a way to identify possible

*Corresponding author.
javier.landaeta@cpfs.mpg.de
†Corresponding author.
elena.hassinger@cpfs.mpg.de

triplet states since H_P should depend on the orientation of the applied magnetic field with respect to the direction of the spins of the Cooper pairs [4–6]. In experiment, however, the observed angle dependencies of the upper critical fields in the abovementioned systems seem to be dominated by the orbital limit or by the interplay of superconductivity and field-enhanced spin fluctuations associated with an Ising quantum critical point [2,7].

Recently, CeRh$_2$As$_2$ was discovered to have unique and highly anisotropic superconducting critical field phase diagrams [Figs. 4(a) and 4(f)], with a suggested field-induced odd-parity state [8]. The aim of this study is to investigate its angle dependence in detail in order to find out more about the superconductivity itself and its relation with the normal state.

CeRh$_2$As$_2$ is a heavy-fermion compound with an electronic specific heat coefficient close to 1 J/mol K^2 at 0.5 K. At $T_0 \approx 0.4$ K, a phase transition to a suggested quadrupole-density-wave (QDW) state occurs [9]. At $T_c = 0.26$ K, CeRh$_2$As$_2$ enters a low-field superconducting state (SC1). A magnetic field applied along the c axis induces a transition at $\mu_0 H^* \approx 4$ T into a second high-field superconducting state

SC2, with an upper critical field $H_{c2} = 14$ T. T_0 is suppressed at approximately 4 T. For in-plane fields, only the low-field state SC1 appears, with $H_{c2} = 2$ T. T_0 increases with field for this field direction. Furthermore, in zero field within the SC state a broadening of the As(2) nuclear quadrupole resonance line was interpreted as the onset of antiferromagnetic (AFM) order [10]. However, no additional anomaly was detected in the bulk measurements such as specific heat and thermal expansion [8,9].

The crystal structure of $CeRh_2As_2$ is centrosymmetric, but the inversion symmetry is broken locally at the Ce sites enabling a Rashba spin-orbit coupling with alternating sign on neighboring Ce layers [8]. Assuming dominant intralayer singlet SC pairing, a c-axis field transforms an even-parity superconducting state with equal gap sign on both Ce layers into an odd-parity one with alternating gap sign [8,11]. The latter may be topological [12,13] and can be described as a pseudospin triplet state with $\vec{d}$ vector in the plane leading to the absence of a Pauli limit for $H\|c$ [8,14].

The unusual results for the field along the c axis may also have another origin. One possibility emerged from the observation that the QDW state below $T_0 \approx 0.4$ K is suppressed by a c-axis field of similar strength as H^* [8,9,15]. So, the SC1 phase is found to be embedded in the QDW phase for both field directions, but the SC2 phase would be outside the QDW phase. The presence of absence of the QDW state might explain the difference of the superconducting properties and in particular of H_{c2} between the SC1 and SC2 states [8]. Ignoring the QDW and AFM phases, other possibilities have been suggested to explain the origin of the SC1 and SC2 phases as a change between different superconducting order parameters [12,16,17]. There are scenarios which involve a field-driven Fermi-surface Lifshitz transition [18] or the presence of a field-induced quantum critical point [2,7]. Eventually, because the normal state is also anisotropic, a study of the angle dependence of the superconducting states is a promising way to distinguish between those scenarios.

Hence, we study the superconducting phase diagram as a function of magnetic field direction using thermodynamic techniques. We find that the angle dependence supports the picture that SC2 is an odd parity state with pseudospin $\vec{d}$ vector in the plane. $CeRh_2As_2$ seems to be the first compound where the anisotropy of the Pauli limiting can be used to reveal triplet superconductivity.

II. RESULTS

In the following, we show results of ac susceptibility χ_{ac}, magnetic torque τ, and specific heat C as a function of temperature and magnetic field in different directions with an angle θ away from the c axis. These probes were chosen because they are sensitive to the bulk properties of the material and they can detect the transition inside the superconducting state [8]. Previously it was found that the T_c from resistivity is higher than the bulk T_c from

specific heat or low-frequency ac susceptibility [8]. It was suggested that this is due to percolating strain-induced superconductivity around impurities. Experimentally, the resistive T_c follows the bulk T_c in a parallel fashion for both $H\|c$ and $H\|a$ [9,19]. While the angle dependence of the superconducting state could have been investigated by resistivity as well, the transition at H^* is invisible to this probe [8,9,19].

Figure 1(a) shows the magnetic field dependence of χ_{ac} at the temperature of 45 mK for different angles. Details on the experimental methods can be found in Ref. [20]. We measured from $\theta = 0°$ ($H\|c$) to $90°$ ($H\perp c$ here named $H\|ab$). The in-plane field orientation was [110] for torque but not defined for χ_{ac} and C/T. A small but clear signature of the transition between SC1 and SC2 named H^* appears for angles below $35°$. At $30°$ a small anomaly is visible at H^* in the derivative $d\chi_{ac}/dH$ highlighted in the inset of Fig. 1(a).

We define the upper critical field H_{c2} at the onset of the diamagnetic transition in order to be consistent with the previous analysis [8] [horizontal dashed line in Fig. 1(a)] and H^* at the maximum of the small bump in the field dependence of χ_{ac}. The torque τ is shown in Figs. 1(b) and 1(c). As expected, its field dependence depicted in the inset of Fig. 1(b) is quadratic in field in the normal state. Since we are interested in deviations from this behavior in the superconducting state, we present data as τ/H^2 and scaled by $\sin(2\theta)^{-1}$, which is the standard angle dependence of torque. It displays a similar steplike feature at H^*. The strong hysteresis loop in the superconducting state was already observed in the magnetization in $CeRh_2As_2$ [8,20]. While the hysteresis is counterclockwise at small angles [inset of Fig. 1(b)], as in the magnetization, it changes to clockwise at higher angles [Fig. 1(b)]. This is related to a change in the magnetization anisotropy (see Ref. [20]). H_{c2} is defined in the torque at the field where up and down sweep curves start to separate. Since this happens rather smoothly for small angles, there is a larger uncertainty on these points. Strictly speaking, this is the so-called "irreversibility field." As usually observed, it is slightly lower than H_{c2} from χ_{ac}, but it follows its angle dependence.

For fields near the in-plane direction, an additional transition is observed at $H_{cr} \approx 9$ T [inset of Fig. 1(c) and Ref. [20]]. Previously, this transition was associated with a change of the order below T_0 [9]. H_{cr} increases when the field is turned away from the ab plane toward the c axis until, for angles below $58°$, this anomaly cannot be resolved experimentally any more. As can be seen in the inset of Fig. 1(c), it is strongly hysteretic indicating a first-order transition, in agreement with results from resistivity and magnetostriction [9]. No further transitions have been detected for in-plane fields up to 36 T and c-axis fields up to 26 T [20].

From these data we find the angle dependence of H_{c2}, H^*, and H_{cr} shown in Fig. 2(a). Here, the upper critical field H_{c2} decreases rapidly as the angle is increased with
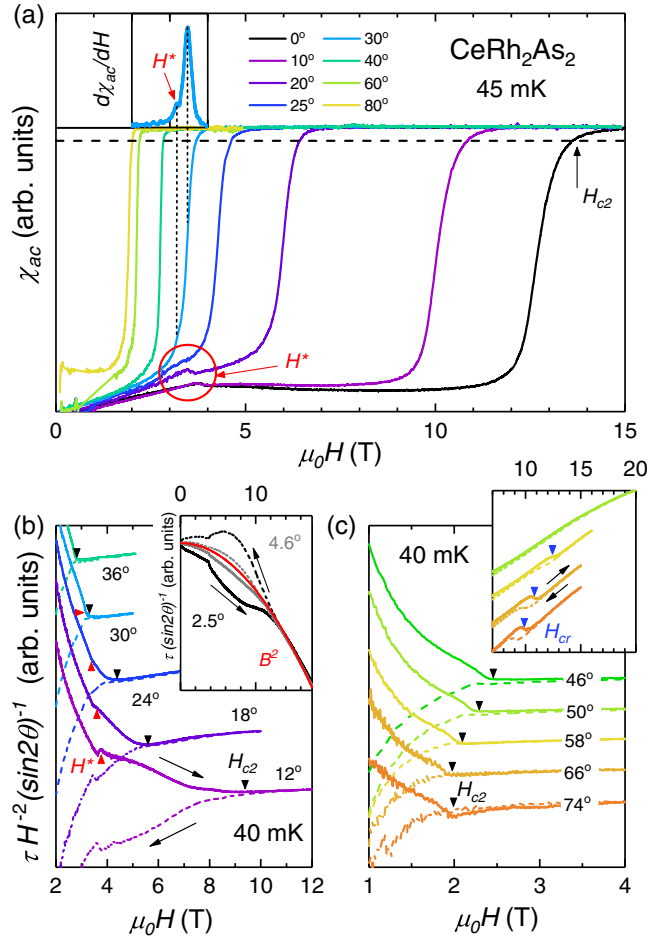
FIG. 1. Magnetic field dependence of magnetic susceptibility and torque for different field directions. (a) Magnitude of the ac susceptibility χ_{ac} at 45 mK for different angles as indicated. $\theta = 0°$ corresponds to $\mu_0 H \| c$. The bump labeled as H^* is the transition between SC1 and SC2. The inset shows the derivative of the curve at 30°, indicating that H^* is still present at that angle. The dashed horizontal line indicates the value at which H_{c2} is defined. (b) Magnetic torque divided by $H^2 \sin(2\theta)$ at 40 mK. The inset shows the torque for 2.5° and 4.6° where the hysteresis of τ at low angles is visible. Additionally, the red line gives the expected B^2 dependence. (c) Torque divided by $H^2 \sin(2\theta)$ for angles close to the plane. The inset in (c) shows the additional phase transition appearing at $H_{cr} \approx 9$ T. In (b) and (c) curves are shifted for clarity.

respect to the c axis until it approaches the value of H^* at about 35°. From this point on, we only detect one superconducting state in which the H_{c2} slowly decreases with angle until it reaches the expected value of ≈ 2 T for $H \| ab$.

For different magnetic field angles, temperature-dependent ac susceptibility (data in Ref. [20]) and specific heat were measured in magnetic field. A selection of the specific heat data is depicted in Fig. 3, where a nuclear contribution has been removed. In this paper, these data are used to extract the superconducting transition temperatures and a qualitative behavior of T_0 (see below). A more

detailed analysis of the specific heat and the angle dependence of T_0 is the subject of future studies.

The superconducting critical field phase diagrams are shown in Fig. 4, where data from the temperature sweeps in Fig. 3 and from Ref. [20] and from the field sweeps in Fig. 1 are included. Note that the discrepancy between the critical field from specific heat and ac susceptibility at 20° is ascribed to a difference in angle within the uncertainty because in this angle region, H_{c2} changes strongly even with only a few degrees. For all angles below 35°, a kink appears in $H_{c2}(T)$ at a field that is close to H^* obtained from the field sweeps revealing that the H^* line is almost temperature independent for all angles. As already observed for the high-symmetry directions [8], the phase diagrams determined by ac susceptibility are fully consistent with those obtained from the specific heat and hence reveal the bulk properties.

The present torque and specific heat data also provide some new information on the phase diagram of the phase connected with T_0 which was identified with a QDW order [8,9]. An order of magnetic dipoles was ruled out since magnetic probes like ac susceptibility or magnetization do not display any signature at this transition [8]. On the other hand, the small hump in the specific heat and a clear jump in the thermal expansion reveal a bulk phase transition. The electrical resistivity shows an increase below T_0 possibly due to nesting. This indicates that itinerant f electrons forming the bands at the Fermi energy are involved in the T_0 order. The field dependence of T_0 is extremely anisotropic. For in-plane fields, an increase of T_0 is observed [8,9]. Since such an increase is typical for local quadrupolar order in cubic systems, it was one of the signs that the T_0 order involves quadrupolar degrees of freedom of the itinerant electrons that are induced by a Kondo mixing with the crystal electric field doublets. This idea was supported by calculations of the quadrupole moment for such a system [9]. Furthermore, at $\mu_0 H_{cr} = 9$ T, a first-order transition to another state occurs. In contrast, for c-axis fields, the T_0 order is suppressed at roughly $H_0 = (4 \pm 1)$ T, seemingly coincident with the transition inside the superconducting state [8]. Both H_0 and H_{cr} present a clear angle dependence. For 10° and 20°, the hump at T_0 is suppressed with field, but remains visible up to roughly 4 T [Figs. 3(a) and 3(b)], similar to what was observed for $H \| c$ [8]. For 45°, T_0 stays approximately constant in applied fields up to 10 T [Fig. 3(c)], far above the superconducting critical field, similar to the behavior observed for $H \| ab$ [8,9]. Therefore, H_0 stays roughly constant at least up to 20° and then starts increasing strongly for angles between 20° and 45°. Furthermore, because H_{cr} shoots up for angles from 90° to 58°, it might meet the H_0 line in a tricritical point in the range $30° < \theta < 60°$ and $\mu_0 H > 15$ T. Another possibility is that the H_{cr} transition ends in a critical end point, since the anomaly just disappears going from 58° to 50°. The absence of any further anomaly in the torque up to
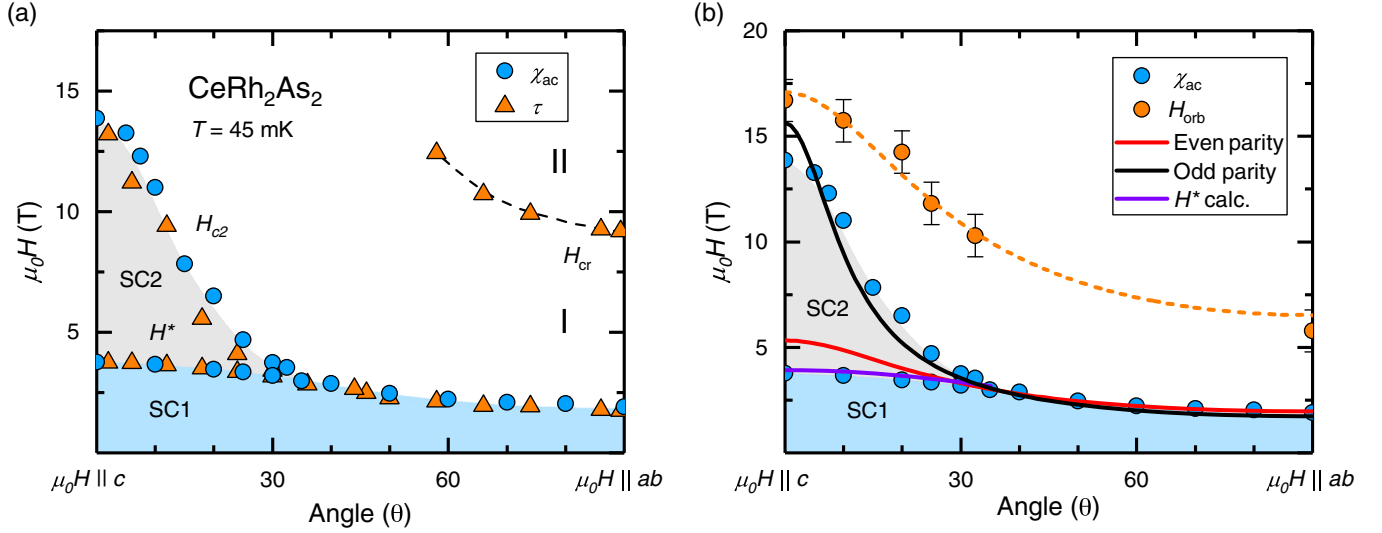
FIG. 2. Angle dependence of the critical fields at 45 mK. (a) Different symbols represent different experimental techniques as indicated. H_{cr} indicates a transition between two ordered states I and II [9]. Since it shows a strong hysteresis, only the critical fields from up sweeps are shown here. The critical fields from the down sweeps are typically around 1 T lower. (b) Angle dependence of the upper critical fields of SC1 and SC2 as well as the orbital limit H_{orb} of SC1 obtained from the phase diagrams in Fig. 4 and a fit of it using Eq. (1) (orange dashed line). Red and black lines are fits to Eq. (2) at 45 mK, and the violet line reflects the calculated H^*, as detailed in the main text and Ref. [20].

$\mu_0 H = 36$ T for $\theta = 89.4°$ ($H\|a$) [20] indicates that the phase forming at $H > H_{cr}$ is stable until very high field as observed, e.g., for the quadrupolar phase II in CeB_6 in high magnetic fields [21]. Further high-field studies are necessary to determine the H_0 boundary. Notably, the angle dependence of H_0 and H_{cr} are quite different from those of H_{c2}, suggesting the interaction between this phase and superconductivity to be weak. On the other hand, for low angles, H_0 nearly coincides with H^* up to 20°.

Let us now concentrate on the angle dependence of the critical field of the state SC1. Previous analysis along the two crystallographic directions showed that the orbital limit H_{orb} in $CeRh_2As_2$ is large and strongly exceeds the experimental critical fields of SC1. Therefore, this state is strongly Pauli limited with enhanced Pauli fields compared to the bare weak coupling value of $\mu_0 H_P = 1.84T_c \approx 0.5$ T [22,23]. We now proceed with the determination of the angle dependence of both the orbital limit H_{orb} and the Pauli limit H_P. In the clean limit H_{orb} is given by the slope
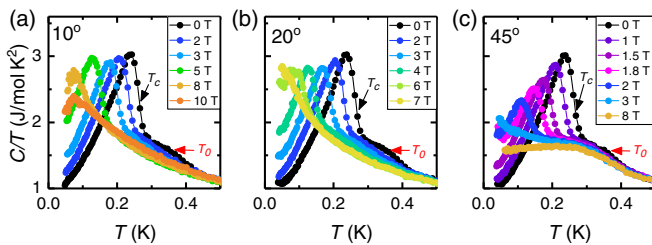

FIG. 3. (a)–(c) Temperature dependence of the specific heat C/T in magnetic field at different angles. Here, a nuclear contribution has been removed [20].

of the critical field $H_{c2}(T)$ near T_c as $\mu_0 H_{orb}(T = 0) = -0.73T_c(dH_{c2}/dT)|_{T=T_c}$ [24].

From the data in Fig. 4 we extract the values of the H_{c2} slopes near T_c [20] and, hence, H_{orb} for all angles, which are given in Fig. 2(b). We observe that T_c varies slightly even in zero field for different sample orientations, which is probably due to the remanent magnetic field in the superconducting magnet and slightly different shapes of the ac susceptibility curves at different angles near the onset of the transition where we define T_c. The values of T_c are listed in Ref. [20]. Note that the uncertainty of the slope and hence H_{orb} at each angle is quite large [error bars in Fig. 2(b)].

The angle dependence of H_{orb} behaves as expected for an anisotropic bulk superconductor [25] according to

$$H_{c2}(\theta) = \frac{H_{c2}^c}{\sqrt{\Gamma^2 \sin\theta^2 + \cos\theta^2}}, \qquad (1)$$

where the anisotropy parameter $\Gamma = H_{c2}^c/H_{c2}^{ab}$. We find $\Gamma = H_{orb}^c/H_{orb}^{ab} = 2.6$ and $\mu_0 H_{orb}^c = 16.2$ T as shown by the dashed orange line in Fig. 2(b). For a fully gapped 3D superconductor in the Bardeen-Cooper-Schrieffer theory, this angle dependence reflects the anisotropy of the normal state since $\mu_0 H_{orb} = \Phi_0/2\pi\xi^2(T)$ and $\xi(0) = 0.18\hbar v_F/k_B T_c$. Using $v_F = \hbar k_F/m^*$, we find $H_{orb}^c/H_{orb}^{ab} = m_a^{*2}/m_c^* m_a^* \Rightarrow m_a^*/m_c^* = 2.6$. This is comparable to the weak anisotropy in the magnetization at 2 K, where the in-plane value is a factor of 2 larger than the c-axis value [8]. It will be interesting to see if band-structure calculations confirm this anisotropy in the future [9].
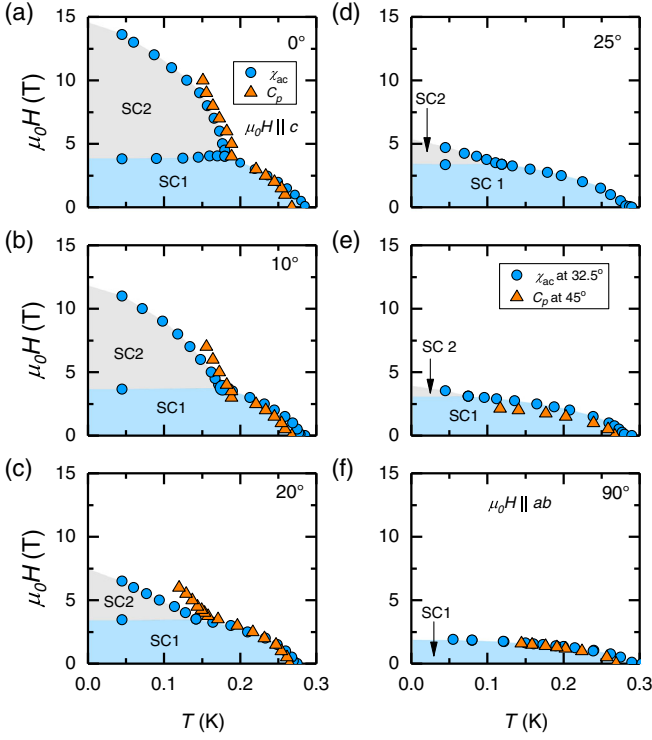
FIG. 4. (a)–(f) Magnetic field-temperature phase diagrams of $CeRh_2As_2$ for different directions of the magnetic field. The experimental points are from ac susceptibility and specific heat, as indicated. The data shown in (a) and (f) were taken from Ref. [8].

As a next step, the Pauli paramagnetic limit of SC1 is investigated. Here, we consider the following expression for the upper critical field of a spin-singlet superconductor with both orbital and Pauli limiting,

$$\ln(t) = \int_0^\infty du \left\langle \frac{[1 - F_\theta + F_\theta \cos(\frac{H g_\theta u}{H_P t})] \exp(\frac{-Hu^2}{\sqrt{2} H_{orb} t^2}) - 1}{\sinh u} \right\rangle,$$

(2)

where g_θ is a field-angle-dependent g factor, $t = T/T_c$, and $F_\theta = 1$ quantifies the pair breaking due to Pauli limiting (as discussed later, this takes a different form for a pseudospin-triplet order parameter). $\langle \cdots \rangle$ indicates an angular average around the Fermi surface. Using the H_{orb} values from the fit of its angle dependence (in order to reduce the uncertainty at each angle), we find that H_P/g_θ exhibits an anisotropy similar to $H_{c2}(\theta)$, that has the angular dependence given by Eq. (1) with anisotropy parameter $\Gamma_g = 2.8$. For more details about the fitting procedure, refer to Ref. [20]. Within error bars, there is no temperature dependence of the H_{c2} anisotropy for SC1.

Now let us turn to the critical field of SC2 with the aim to understand what is causing the strong suppression of H_{c2} when fields are turned away from the c axis and the disappearance of SC2 at an angle of 35°. For $H \| c$, the

temperature dependence of H_{c2} follows qualitatively—and even quantitatively, when a lower T_c is assumed—very well the expectations for a pure orbital limit [8] without Pauli-limiting effect [20].

To first order, the orbital limit of SC2 should be similar to the one of SC1 given in Fig. 2(b) [26]. Therefore, we can make the first statement that the angle dependence of the orbital limit is not strong enough to describe the steep decrease of the experimental critical field H_{c2} with angle. Hence, the decrease must be related to the Pauli limiting kicking in when the field is tilted toward the ab plane. As discussed in the context of SC1, one place where the Pauli field introduces anisotropy is through the spin-orbit coupling renormalized g factor g_θ. However, this anisotropy is also too small to account for the steep decrease of the experimental critical field H_{c2} with angle since any renormalized H_P for a spin-singlet state should have the same anisotropy as the one observed in SC1. Consequently, there must be another source of anisotropy due to Pauli limiting. Indeed, this is exactly the behavior expected for triplet superconductors with $\vec{d}$ vector in the plane (helical state): an absence of Pauli limiting for $H \| c$ (infinite H_P^c) and presence of Pauli limiting for $H \| ab$ which is isotropic in the plane. The latter is enhanced compared to the bare value [8,27], when Rashba spin-orbit coupling is included. Here, we consider such a helical triplet state subject to an orbital critical field, for which the critical field is given by the expression of Eq. (2) but now with $F_\theta = |\hat{d} \cdot \hat{h}_\theta|^2$, where $\hat{d}$ is $\vec{d}/|\vec{d}|$ and $\hat{h}_\theta$ is a unit vector that gives the direction of the Zeeman field projected onto to the pseudospin basis [8]. As long as the orbital field energy ($g_\theta \mu_B H_{orb}$) is smaller than the spin-orbit coupling energy, this is the expression for the odd-parity spin-singlet state in which the order parameter has opposite sign on the two inequivalent Ce layers. In Fig. 2(b), we show the calculated critical field for the state SC2. In Ref. [20], we provide plots of the calculated H-T phase diagrams for the different field angles. The agreement with experiment is excellent. Note that even the angle above which only one SC phase occurs is reproduced.

This leads us to the main conclusion of our paper: The angle dependence of the superconducting critical field is dominated by the huge anisotropy of the Pauli field of an odd-parity state with d vector in the plane, in agreement with the interpretation in Ref. [8] and in previous models of locally noncentrosymmetric SC [14], although here the SC state is a pseudospin-triplet state with staggered dominant singlet intralayer pairing.

As a final point, we have also calculated H^*, the first-order transition between the SC1 and SC2 states. In the previous study for $H \| c$, the H^* transition was found to be a result of a competition between the Pauli-limited SC1 (with Pauli field $H_{P,1}$) and the Pauli-limit-free SC2, so that $H^* \lesssim H_{P,1}$ [8]. Here, we calculate the phase transition between SC1 and SC2 for all magnetic field directions from the free energies taking only the Pauli-limiting effect into account

[violet line in Fig. 2(b)], with no additional parameters beyond those calculated from the fitting procedure. Neglecting the orbital limit leads to a slight overestimate of the critical field [28], but the angular dependence is in perfect agreement with experiment [20].

III. DISCUSSION

We would like to emphasize that the simple model established in Ref. [8] and extended here to intermediate angles can reproduce all experimental observations based on only 3 free parameters that cannot be measured experimentally: the critical temperature of the superconducting state SC2 $T_{c,2}$, the in-plane Pauli limit $H_{P,1}$, and the strength of the Rashba spin-orbit coupling relative to the interlayer hopping $\tilde{\alpha}$. This model has the minimal number of bands in this crystal symmetry and naturally contains both even and odd parity superconducting states. Even though CeRh$_2$As$_2$ certainly contains multiple bands [9], renormalized density functional theory calculations reveal the bulk of the density of states to be on symmetry-related Fermi surfaces near the zone boundary—which justifies the single-band approach used here [9,29].

The angle dependence of the orbital limit of SC1 corroborates a rather 3D Fermi surface in agreement with the strongly warped cylinders calculated with renormalized band-structure calculations [9]. Both the anisotropy of the effective mass given by the anisotropy of $H_{\rm orb}$ as well as the anisotropy of the g factor (and the magnetic susceptibility) are rather small. Furthermore, in quasi-2D systems such as Sr$_2$RuO$_4$ [30], CeCoIn$_5$ [31], or FeSe [32], the critical field is usually larger for in-plane fields than for c-axis fields, because orbital motion perpendicular to the layers is hindered and almost no orbital limiting occurs with large $H_{\rm orb}$ for in-plane fields. In the 2D limit a cusp is expected for $H_{\rm orb}$ for fields close to the a axis as observed, for example, in FeSe, K$_2$Cr$_3$As$_3$, or in superlattices of CeCoIn$_5$/YbCoIn$_5$ [25,32–34], but not observed here. A previous theoretical study found that going from a quasi-two-dimensional Fermi surface to a three-dimensional Fermi surface reduces the anisotropy of SC1 due to Rashba spin-orbit coupling, but should not affect qualitatively the anisotropy of SC2 for the suggested scenario here [12]. However, they investigated a Fermi surface at the Brillouin zone center and the situation may change for a Fermi surface at the zone boundary where—due to the nonsymmorphic structure and symmetry-imposed degeneracies—large values of the Rashba strength over interlayer coupling are expected [29].

In ferromagnetic superconductors, which are the most prominent candidates of spin-triplet superconductivity, the critical fields are highly anisotropic [2,35], and the strong enhancements observed along certain directions or in the field-reentrant phases are related with strong Ising-type spin fluctuations and quantum criticality influencing the orbital limit [2,7]. Here, we find that this is not the case for

CeRh$_2$As$_2$, where the anisotropy is accounted for by a pseudospin $\vec{d}$ that is oriented in the basal plane. An interesting open issue is why the orbital critical field and the Sommerfeld coefficient are so large for CeRh$_2$As$_2$. In the noncentrosymmetric superconductors CePt$_3$Si and CeRhSi$_3$, the origin of this was proposed to be antiferromagnetic quantum critical fluctuations that enhance the electron effective mass [7,36–39]. This needs to be investigated further in CeRh$_2$As$_2$, where quadrupolar as well as antiferromagnetic degrees of freedom are suggested to play a role [9,10,40]. CeIrSi$_3$, CeRhSi$_3$, and CeCoGe$_3$ show a similar anisotropy of the superconducting state to CeRh$_2$As$_2$ with absence of Pauli limit for $H\|c$ and strong but enhanced Pauli limit for $H\|ab$ [37,41,42], but a full determination of the angle dependence has not been possible yet because the large anisotropy appears only under pressure, preventing an easy angle-dependent measurement.

At this point, we would like to discuss the possibility that the transition between the two superconducting states might originate from the suppression of the T_0 order [9,15] or of the AFM order [10] by a field along the c axis. In the former scenario, the suppression of the T_0 order is considered to be responsible for the H^* transition line and the superconducting order parameter remains the same in the SC1 and SC2 states, i.e., below and above H^*. Our results indicate that whenever the superconducting state coexists with the T_0 order, it is Pauli limited, but when T_0 is suppressed for fields larger than $\mu_0 H^* \approx 4$ T, the superconducting state is not any more, or much less, Pauli limited. Knowing that the T_0 order probably causes a nesting, i.e., partial gapping of the Fermi surface, it seems natural that it might affect the superconducting state. Accordingly, in order to understand the observed anisotropy of the superconducting state in this paper, the T_0 order would, at least, have to suppress the spin-orbit coupling, for example, by gapping out parts of the Fermi surface with large spin-orbit coupling. However, this seems difficult to explain microscopically, as it would imply that the bare spin-orbit coupling is significantly larger than the already substantial spin-orbit coupling used to fit the critical field data in Fig. 2. In the latter scenario, the AFM order is considered to be responsible for the H^* line. The behavior of the AFM state with magnetic field and angle is not known yet, besides a single nuclear magnetic resonance measurement showing a line broadening starting between 0.2 and 0.3 K at 1.4 T along the c axis (see Supplemental Material of Ref. [10]). The AFM order is expected to be suppressed by the magnetic field, and the angle dependence of this suppression might be similar to the H^* line. However, with a transition temperature of $T_N \approx 0.25$ K in zero field, it seems very unlikely that the suppression of T_N would be responsible for the transition line at $\mu_0 H^* = 4$ T. In fact, this would imply T_N to be almost constant up to 4 T followed by a first-order phase transition. While such behavior is unexpected, it has been observed,

e.g., in systems which are near a ferromagnetic quantum critical point and show field-induced tricritical points, like $Yb(Rh_{1-x}Co_x)_2Si_2$ with $x = 0.18$ [43]: In this material the zero-field AFM phase decreases only very little with field along the c axis, and then a first-order transition to a polarized state occurs. However, the underlying physics of this system is different, since it is antiferromagnetic but very close to a ferromagnetic state with an extremely large magnetocrystalline anisotropy of ≈ 10. In $CeRh_2As_2$ the susceptibility is too small to be close to ferromagnetism and the magnetocrystalline anisotropy is only $\lesssim 2$. So it is unlikely that similar physics is at play in $CeRh_2As_2$.

Although the angle dependence cannot completely rule out these scenarios, a transition between two superconducting states seems more natural, especially given how well it fits the data.

IV. CONCLUSION

The excellent agreement of the model with the experimental results strengthens the interpretation that the superconducting state changes from even to odd parity at H^* and that the strong anisotropy of the critical field is rooted in the Pauli-limiting effect of a helical pseudospin d vector. Since other orders are not included in this model and are not needed to obtain the good agreement, their influence on the superconducting phase diagram and especially on H^* appears to be small. However, this point can only be resolved and other scenarios ruled out when more microscopic information on the orders and on the pairing mechanism are available in the future, so that their interplay can be investigated and understood.

ACKNOWLEDGMENTS

[1] R. A. Fisher, S. Kim, B. F. Woodfield, N. E. Phillips, L. Taillefer, K. Hasselbach, J. Flouquet, A. L. Giorgi, and J. L. Smith, *Specific Heat of* UPt_3: *Evidence for Unconventional Superconductivity*, Phys. Rev. Lett. **62**, 1411 (1989).

[2] Dai Aoki, Kenji Ishida, and Jacques Flouquet, *Review of U-Based Ferromagnetic Superconductors: Comparison between UGe2, URhGe, and UCoGe*, J. Phys. Soc. Jpn. **88**, 022001 (2019).

[3] S. Ran, C. Eckberg, Q.-P. Ding, Y. Furukawa, T. Metz, S. R. Saha, I.-L. Liu, M. Zic, H. Kim, J. Paglione, and N. P. Butch, *Nearly Ferromagnetic Spin-Triplet Superconductivity*, Science **365**, 684 (2019).

[4] M. Sigrist, *Introduction to Unconventional Superconductivity*, AIP Conf. Proc. **789**, 165 (2005).

[5] K. Machida, T. Ohmi, and M.-A. Ozaki, *Anisotropy of Upper Critical Fields for d- and p-Wave Pairing Superconductivity*, J. Phys. Soc. Jpn. **54**, 1552 (1985).

[6] V. P. Mineev and K. Samokhin, *Introduction to Unconventional Superconductivity* (Taylor & Francis, London, 1999).

[7] Y. Tada, N. Kawakami, and S. Fujimoto, *Upper Critical Field in Superconductors near Ferromagnetic Quantum Critical Points: UCoGe*, J. Phys. Soc. Jpn. **80**, SA006 (2011).

[8] S. Khim, J. F. Landaeta, J. Banda, N. Bannor, M. Brando, P. M. R. Brydon, D. Hafner, R. Küchler, R. Cardoso-Gil, U. Stockert, A. P. Mackenzie, D. F. Agterberg, C. Geibel, and E. Hassinger, *Field-Induced Transition within the Superconducting State of* $CeRh_2As_2$, Science **373**, 1012 (2021).

[9] D. Hafner, P. Khanenko, E.-O. Eljaouhari, R. Küchler, J. Banda, N. Bannor, T. Lühmann, J. F. Landaeta, S. Mishra, I. Sheikin, E. Hassinger, S. Khim, C. Geibel, G. Zwicknagl, and M. Brando, *Possible Quadrupole Density Wave in the Superconducting Kondo Lattice* $CeRh_2As_2$, Phys. Rev. X **12**, 011023 (2022).

[10] M. Kibune, S. Kitagawa, K. Kinjo, S. Ogata, M. Manago, T. Taniguchi, K. Ishida, M. Brando, E. Hassinger, H. Rosner, C. Geibel, and S. Khim, *Observation of Antiferromagnetic Order as Odd-Parity Multipoles inside the Superconducting Phase in* $CeRh_2As_2$, Phys. Rev. Lett. **128**, 057002 (2022).

[11] T. Yoshida, M. Sigrist, and Y. Yanase, *Pair-Density Wave States through Spin-Orbit Coupling in Multilayer Superconductors*, Phys. Rev. B **86**, 134514 (2012).

[12] A. Skurativska, M. Sigrist, and M. H. Fischer, *Spin Response and Topology of a Staggered-Rashba Superconductor*, Phys. Rev. Research **3**, 033133 (2021).

[13] Kosuke Nogaki, Akito Daido, Jun Ishizuka, and Youichi Yanase, *Topological Crystalline Superconductivity in Locally Noncentrosymmetric* $CeRh_2As_2$, Phys. Rev. Research **3**, L032071 (2021).

[14] T. Yoshida, M. Sigrist, and Y. Yanase, *Parity-Mixed Superconductivity in Locally Non-Centrosymmetric System.*, J. Phys. Soc. Jpn. **83**, 013703 (2014).

[15] P. Khanenko *et al.* (to be published).

[16] D. Möckli and A. Ramires, *Two Scenarios for Superconductivity in* $CeRh_2As_2$, Phys. Rev. Research **3**, 023204 (2021).

[17] David Möckli and Aline Ramires, *Superconductivity in Disordered Locally Noncentrosymmetric Materials: An Application to* $CeRh_2As_2$, Phys. Rev. B **104**, 134517 (2021).

[18] A. Ptok, K. J. Kapcia, P. T. Jochym, J. Łażewski, A. M. Oleś, and P. Piekarz, *Electronic and Dynamical Properties of* $CeRh_2As_2$: *Role of* Rh_2As_2 *Layers and Expected Orbital Order*, Phys. Rev. B **104**, L041109 (2021).

[19] S. Onishi, U. Stockert, S. Khim, J. Banda, M. Brando, and E. Hassinger, *Low-Temperature Thermal Conductivity of the Two-Phase Superconductor* $CeRh_2As_2$, Front. Electro. Mater. **2** (2022).

[20] See Supplemental Material at http://link.aps.org/supplemental/10.1103/PhysRevX.12.031001 for a description of experimental methods, the full datasets of ac susceptibility and torque, and details on the theoretical model.

[21] J. M. Effantin, J. Rossat-Mignod, P. Burlet, H. Bartholin, S. Kunii, and T. Kasuya, *Magnetic Phase Diagram of* CeB_6, J. Magn. Magn. Mater. **47,48**, 145 (1985).

[22] A. M. Clogston, *Upper Limit for the Critical Field in Hard Superconductors.*, Phys. Rev. Lett. **9**, 266 (1962).

[23] B. S. Chandrasekhar, *A Note on the Maximum Critical Field of High-Field Superconductors*, Appl. Phys. Lett. **1**, 7 (1962).

[24] E. Helfand and N. R. Werthamer, *Temperature and Purity Dependence of the Superconducting Critical Field, H_{c2}. II*, Phys. Rev. **147**, 288 (1966).

[25] M. Tinkham, *Introduction to Superconductivity* (McGraw-Hill, New York, 1996), Vol. 2.

[26] Note that this is true only if both SC states live on the same Fermi surface since H_{orb} depends mainly on the Fermi velocity. If different Fermi surfaces are responsible for SC1 and SC2, the anisotropy of H_{orb} of SC2 and SC1 could be different. In addition, the orbital limit can also strongly depend on the nodal structure of the gap function [7]; this is currently unknown for $CeRh_2As_2$.

[27] P. A. Frigeri, D. F. Agterberg, A. Koga, and M. Sigrist, *Superconductivity without Inversion Symmetry: MnSi versus* $CePt_3Si$, Phys. Rev. Lett. **92**, 097001 (2004).

[28] E. G. Schertenleib, M. H. Fischer, and M. Sigrist, *Unusual $H - T$ Phase Diagram of* $CeRh_2As_2$*: The Role of Staggered Noncentrosymmetricity*, Phys. Rev. Research **3**, 023179 (2021).

[29] D. C. Cavanagh, T. Shishidou, M. Weinert, P. M. R. Brydon, and Daniel F. Agterberg, *Nonsymmorphic Symmetry and Field-Driven Odd-Parity Pairing in* $CeRh_2As_2$, Phys. Rev. B **105**, L020505 (2022).

[30] S. Kittaka, T. Nakamura, Y. Aono, S. Yonezawa, K. Ishida, and Y. Maeno, *Angular Dependence of the Upper Critical Field of* Sr_2RuO_4, Phys. Rev. B **80**, 174514 (2009).

[31] Shugo Ikeda, Hiroaki Shishido, Miho Nakashima, Rikio Settai, Dai Aoki, Yoshinori Haga, Hisatomo Harima, Yuji Aoki, Takahiro Namiki, Hideyuki Sato, and Yoshichika Ōnuki, *Unconventional Superconductivity in* $CeCoIn_5$ *Studied by the Specific Heat and Magnetization Measurements*, J. Phys. Soc. Jpn. **70**, 2248 (2001).

[32] L. S. Farrar, M. Bristow, A. A. Haghighirad, A. McCollam, S. J. Bending, and A. I. Coldea, *Suppression of Superconductivity and Enhanced Critical Field Anisotropy in Thin Flakes of FeSe*, npj Quantum Mater. **5**, 29 (2020).

[33] H. Zuo, J.-K. Bao, Y. Liu, J. Wang, Z. Jin, Z. Xia, L. Li, Z. Xu, J. Kang, Z. Zhu, and G.-H. Cao, *Temperature and Angular Dependence of the Upper Critical Field in* $K_2Cr_3As_3$, Phys. Rev. B **95**, 014502 (2017).

[34] S. K. Goh, Y. Mizukami, H. Shishido, D. Watanabe, S. Yasumoto, M. Shimozawa, M. Yamashita, T. Terashima, Y. Yanase, T. Shibauchi, A. I. Buzdin, and Y. Matsuda, *Anomalous Upper Critical Field in* $CeCoIn_5/YbCoIn_5$ *Superlattices with a Rashba-Type Heavy Fermion Interface*, Phys. Rev. Lett. **109**, 157006 (2012).

[35] D. Aoki, T. Matsuda, V. Taufour, E. Hassinger, G. Knebel, and J. Flouquet, *Extremely Large and Anisotropic Upper Critical Field and the Ferromagnetic Instability in UCoGe*, J. Phys. Soc. Jpn. **78**, 113709 (2009).

[36] N. Kimura, K. Ito, K. Saitoh, Y. Umeda, H. Aoki, and T. Terashima, *Pressure-Induced Superconductivity in Noncentrosymmetric Heavy-Fermion* $CeRhSi_3$, Phys. Rev. Lett. **95**, 247004 (2005).

[37] N. Kimura, K. Ito, H. Aoki, S. Uji, and T. Terashima, *Extremely High Upper Critical Magnetic Field of the Noncentrosymmetric Heavy Fermion Superconductor* $CeRhSi_3$, Phys. Rev. Lett. **98**, 197001 (2007).

[38] I. Sugitani, Y. Okuda, H. Shishido, T. Yamada, A. Thamizhavel, E. Yamamoto, T. D. Matsuda, Y. Haga, T. Takeuchi, R. Settai, and Y. Ōnuki, *Pressure-Induced Heavy-Fermion Superconductivity in Antiferromagnet* $CeIrSi_3$ *without Inversion Symmetry*, J. Phys. Soc. Jpn. **75**, 043703 (2006).

[39] E. Bauer and M. Sigrist, *Non-Centrosymmetric Superconductors: Introduction and Overview*, Lecture Notes in Physics, Vol. 847 (Springer-Verlag, Berlin, 2012).

[40] S. Kitagawa, M. Kibune, K. Kinjo, T. Manago, M.and Taniguchi, K. Ishida, M. Brando, E. Hassinger, C. Geibel, and S. Khim, *Two-Dimensional XY-Type Magnetic Properties of Locally Noncentrosymmetric Superconductor* $CeRh_2As_2$, J. Phys. Soc. Jpn. **91**, 043702 (2022).

[41] R. Settai, Y. Miyauchi, T. Takeuchi, F. Lévy, I. Sheikin, and Y. Ōnuki, *Huge Upper Critical Field and Electronic Instability in Pressure-Induced Superconductor* $CeIrSi_3$ *without Inversion Symmetry in the Crystal Structure*, J. Phys. Soc. Jpn. **77**, 073705 (2008).

[42] M.-A. Méasson, H. Muranaka, T. Kawai, Y. Ota, K. Sugiyama, M. Hagiwara, K. Kindo, T. Takeuchi, K. Shimizu, F. Honda, R. Settai, and Y. Ōnuki, *Magnetic Properties of* $RCoGe_3$ *(R: Ce, Pr, and Nd) and Strong Anisotropy of the Upper Critical Field in Non-Centrosymmetric Compound* $CeCoGe_3$, J. Phys. Soc. Jpn. **78**, 124713 (2009).

[43] S. Hamann, J. Zhang, D. Jang, A. Hannaske, L. Steinke, S. Lausberg, L. Pedrero, C. Klingner, M. Baenitz, F. Steglich, C. Krellner, C. Geibel, and M. Brando, *Evolution from Ferromagnetism to Antiferromagnetism in* $Yb(Rh_{1-x}Co_x)_2Si_2$, Phys. Rev. Lett. **122**, 077202 (2019).